

# DEMONSTRATION OF TEST FACILITY DESIGN OPTIMIZATION WITH THE DYNAMICAL SYSTEM SCALING METHODOLOGY

**Joseph P. Yurko and Cesare Frepoli\***

FPoliSolutions, LLC, 4618 Old William Penn Hwy, Murrysville, PA 15668, USA

\*[frepolc@fpolisolutions.com](mailto:frepolc@fpolisolutions.com)

**Jose N. Reyes, Jr.**

NuScale Power, LLC, 1100 NE Circle Blvd, Suite 200, Corvallis, OR 97330, USA

[jreyes@nuscalepower.com](mailto:jreyes@nuscalepower.com)

## Abstract

The Dynamical System Scaling (DSS) methodology is an innovative new scaling approach that, as the name implies, incorporates the system's dynamic response into the scaling framework. The DSS methodology has the important benefit over the Hierarchical Two-Tiered Scaling (H2TS) and Fractional Scaling Analysis (FSA) methodologies in that scale distortion is a dynamic quantity and can therefore change through time. Additionally, a single integrated distortion measure is computed within the DSS framework rather than computing the distortion measures for each dimensionless group (the Pi-groups) in H2TS. The integrated distortion measure captures the total scale distortion present during the transient. This fact would provide design engineers with a truly new framework for optimizing the design of a test facility. Rather than trying to minimize a potentially large number of distortion measures from H2TS and FSA and accepting tradeoffs where necessary, only the integrated distortion needs to be minimized. This single objective function completely captures how the test facility's response compares to the expected full-scale prototype's response.

This paper demonstrates test facility design optimization within the DSS methodology for a simple single-phase gas depressurization (blowdown) transient. The evaluation model implemented for this task simplifies the interpretation of the results, enabling easy comparison to the H2TS and FSA determined optimal design configurations. However, as simple as the gas blowdown transient is, it still offers challenges representative of those that would be encountered in a real test facility design optimization problem. Namely, multiple time phases which have distinctly different dominant physical phenomena are present in this task. Therefore, the present work requires minimizing the integrated distortion measure within each time phase in order to determine the optimal test facility design.

This paper is one among a series that will compare and contrast the DSS methodology with the H2TS and FSA methods for a variety of practical engineering applications.

**Keywords:** Scaling analysis, dynamical systems, time-dependent scale distortion, H2TS, FSA

## 1. INTRODUCTION

The Dynamical System Scaling (DSS) methodology is a powerful new approach to scaling that as the name implies incorporates the system's dynamic response into the scaling framework [1]. Several other papers within in this Topical Meeting present the DSS formalism [1] and relate DSS to the H2TS and FSA methodologies [2]. This paper briefly summarizes how DSS computes scaling distortion. Therefore an interested reader should consult References [1] and [2] for a detailed theoretical background on DSS.

This paper primarily focuses on applying DSS to a test facility design optimization problem. The transient of interest is a simplified single-phase gas depressurization (blowdown). The prototype facility response is analyzed using DSS which provides a set of similarity criteria that must be satisfied by a test facility. Relationships between the various design variables are determined such that the DSS similarity criteria are satisfied. Because of assumptions used to evaluate the similarity criteria, distortion may still result. The DSS total distortion measure is used as the objective function to find the optimal test facility design.

## 2. SIMILARITY AND SCALING DISTORTION WITH DSS

### 2.1 Dimensionless Coordinates

The coordinates within the DSS framework are the normalized conserved quantity of interest,  $\beta$ , the normalized sum of the agents of change,  $\omega$ , and the process time,  $\tau$ . The normalized sum of the agents of change is simply the time derivative of the normalized response and the process time is equal to  $\tau = \beta/\omega$ .

The coordinates are normalized with respect to the action, which is defined as the final process time minus the initial process time,  $\tau_S = \tau_F - \tau_I$ . The dimensionless quantities that define the state of the system are then:

$$\tilde{\Omega} = \omega\tau_S; \quad \tilde{\beta} = \beta; \quad \tilde{t} = \frac{t}{\tau_S}; \quad \tilde{\tau} = \frac{\tau}{\tau_S} \quad (1)$$

### 2.2 Similarity

The DSS similarity criteria represent how the model's geodesic process curve is transformed relative to the process curve for the prototype. There are a total of five transformations as described in detail in Ref. [1], which are subsets of the general 2-2 affine transformation:

$$\beta_M = \lambda_A \beta_P, \quad \omega_M = \lambda_B \omega_P \quad (2)$$

Applying the above transformations to the governing balance equation, yields the 2-2 affine transformation similarity criteria on the effect parameters as well as associated time scaling:

$$\tilde{\Omega}_R = \lambda_A, \quad \tau_{S,R} = \tau_R = t_R = \frac{\lambda_A}{\lambda_B} \quad (3)$$

Throughout this paper, the subscript P stands for ‘Prototype’, M for ‘Model’ (the test facility) and R for ‘Ratio’ (Model relative to Prototype).

As described in detail in [1], the above similarity criteria satisfy the normalized metric invariance principle:

$$d\tilde{\tau}_M = d\tilde{\tau}_P \quad (4)$$

In words, Eq. (4) states that a differential element of the model’s dimensionless process time equals a differential element of the prototype’s dimensionless process time. If Eq. (4) is satisfied the model’s response is similar to the prototype’s response.

### 2.3 Scaling Distortion

Within DSS, distortion is judged by the concept of geodesic separation between the model and prototype along the dimensionless  $(\beta - \tilde{\Omega} - \tilde{\tau})$  space-time coordinates [1]. The trajectory path the particular response forms over these space-time coordinates is referred to as a process curve. If perfectly scaled, the model’s process curve can be ‘scaled up’ using the DSS transformation parameters to exactly match the prototype’s own process curve. However, if distortion exists, there will be a visible separation between the two. Computing the separation distance between the two process curves quantifies this distortion. Due to the complexities of computing the separation along a curved space-time surface, a flat-space separation distance is presently used to estimate the instantaneous separation at a particular dimensionless process time value:

$$\eta_x(\tilde{\tau}) = \sqrt{1 + \tilde{\tau}^2} \left( \tilde{\Omega}_P(\tilde{\tau}) - \frac{\tilde{\Omega}_M(\tilde{\tau})}{\lambda_A} \right) \quad (5)$$

Reference [2] contrasts the flat-space separation distance to distortion as measured by FSA in more detail. The total separation,  $\eta_T$ , is computed by integrating Eq. (5) from the initial process time,  $\tilde{\tau}_I$ , to the final process time,  $\tilde{\tau}_F$  over the duration of the transient:

$$\eta_T = \frac{1}{\tilde{\tau}_F - \tilde{\tau}_I} \int_{\tilde{\tau}_I}^{\tilde{\tau}_F} |\eta_x(\tilde{\tau})| d\tilde{\tau} \quad (6)$$

The absolute value of the flat-space separation distance is used in Eq. (6) to prevent ‘compensating errors’ from negating each other. Therefore, the total distortion is a single measure that completely accounts for the entire distortion present during the transient. An ideally scaled test facility would have a total distortion measure equal to zero. Since this would not be possible in practice for most transients of interest, the total distortion becomes the objective function to minimize during a test facility design optimization process.

It is important to note that the flat space separation distance computes the difference between the prototype and test facility effect parameters at the same point in dimensionless process time. The test facility and prototype must therefore have the same dimensionless process time interval in order to evaluate the total distortion. If such an ‘overlapping window’ does not exist, then the

flat space separation distance cannot be computed and the full curved-space geodesic separation would be required to evaluate distortion.

### **3. DEMONSTRATION PROBLEM**

#### **3.1 Overview**

Test facility design optimization is demonstrated on a simplified single phase gas blowdown transient. The prototype facility is a cylindrical pressure vessel (tank) filled with air and pressurized to 150 bars at 25°C. The prototype tank is 10 m tall and 1.75 m in diameter. Upon initiation of the transient, the air exits the tank through a discharge valve whose flow area was selected such that the residence time as defined by Reyes and Hochreiter (1998) [3] would be 10 s. Thus, if the initial “break” flow rate was constant the entire tank would empty of air in only 10 s. The resulting discharge valve diameter is 12.37 cm.

The prototype facility is not a real facility, but consists of results generated by simulating the response of the prototype facility just described. The governing equations and phenomena present in the simple simulation tool are discussed in the next section. This work is not trying to compare the predicted results relative to a real experimental test facility. The simplified gas blowdown model is used to illustrate the steps involved to design a real test facility and highlight the important new features that DSS offers designers over conventional scaling methodologies.

The test facility design is specified by several design variables: the height, diameter, break area, initial pressure and initial temperature. The test facility wall thickness is not considered in this work, it is just assumed that the test facility tank can hold whatever the desired initial pressure is. It is also assumed that both the prototype and test facility vent to the same constant ambient pressure of 1 bar. Both facilities effectively vent to volumes much, much larger than their own.

To simplify the analysis slightly, the initial temperature was assumed equal to the prototype initial temperature. The break area will be computed from DSS similarity criteria, defined later on. Therefore, the goal is to find the optimal test facility height, diameter and initial pressure.

A truly optimal design would be one that minimizes both distortion and the cost of the test facility. However, economic considerations were not included in this work. That being said, the physical size and initial pressure provide a representation for the cost, since smaller pressure vessels at reduced pressures would be cheaper to build. Therefore the “optimal” design will be considered one that is “small” and results in a minimal level of distortion as computed by DSS.

#### **3.2 Governing Equations**

The governing equations are assumed to be 0-D lumped parameter mass and energy balance equations on the gas inside the tank. Following Petruzzi et al. (2010) [4] specifically for an ideal gas, the mass and energy balance equations can be reformulated into rate equations on the pressure and temperature response of the gas. Assuming the gas inside the tank has constant specific heats, the resulting balance equations are:

$$\frac{dP}{dt} = -\frac{R\gamma}{V} \dot{m}_{out} T + (\gamma - 1) \frac{\dot{q}_{net}}{V} \quad (7)$$

$$\frac{dT}{dt} = -\frac{(\gamma - 1)}{V} \dot{m}_{out} \frac{RT^2}{P} + (\gamma - 1) \frac{T}{P} \frac{\dot{q}_{net}}{V} \quad (8)$$

### 3.3 Agents of change

There are only two agents of change that act on the system response: the net heat transfer rate, and the energy leaving the break. The net heat transfer rate is due to the heat transfer with the inner tank wall. For simplicity the inner tank wall temperature is assumed to be constant:

$$\dot{q}_{net} = q'' A_{sw} = h_w (T_w - T) A_{sw} \quad (9)$$

Following Petruzzi et al. (2010) [4], the wall heat transfer coefficient only considers natural convective heat transfer. The interested reader should consult that reference for a discussion as to why forced convective heat transfer is neglected. The natural convective heat transfer coefficient is computed using a Nusselt number correlation based on the product of the Grashof and Prandtl numbers (the Rayleigh number):

$$\overline{Nu} = \begin{cases} a (\text{Gr Pr})^b, & \text{Gr Pr} \leq 10^9 \\ c (\text{Gr Pr})^d, & \text{Gr Pr} > 10^9 \end{cases} \quad (10)$$

For laminar flow,  $\text{GrPr} \leq 10^9$ , the correlation parameters are,  $a = 0.555$  and  $b = 1/4$ , while for turbulent flow  $\text{GrPr} > 10^9$ , the parameters are  $c = 0.130$  and  $d = 1/3$ . The wall heat transfer coefficient uses the tank height as the reference length and is defined as:

$$h_w = \frac{\overline{kNu}}{H} \quad (11)$$

The Grashof and Prandtl numbers are evaluated at the film temperature, which is computed as the average between the gas and wall temperatures. For simplicity it was assumed that the gas thermal conductivity and viscosity were constants. The Grashof and Prandtl numbers are:

$$\text{Gr} = \frac{g B_T \rho^2}{\mu^2} H^3 (T_w - T), \quad \text{Pr} = \frac{c_p \mu}{k} \quad (12)$$

The “break” flow rate, is written in terms of the discharge flow area (the “break” flow area) and the break mass flux:

$$\dot{m}_{out} = A_B G_{out} \quad (13)$$

The break mass flux model depends on whether the flow is choked or unchoked. Choked or critical flow occurs when the pressure ratio relative to ambient is below a critical pressure ratio. For an ideal gas with constant specific heats that critical pressure ratio is:

$$r_c = \frac{P_c}{P} = \left( \frac{2}{\gamma + 1} \right)^{\frac{\gamma}{\gamma - 1}} \quad (14)$$

Assuming isentropic flow out the break, the critical mass flux for a single phase ideal gas is:

$$G_c(P, T) = \left[ \gamma \frac{P^2}{RT} \left( \frac{2}{\gamma + 1} \right)^{\frac{\gamma + 1}{\gamma - 1}} \right]^{1/2} \quad (15)$$

The mass flux out the break, including when the flow is unchoked can then be written as [4]:

$$G_{out}(P, T) = \begin{cases} G_c(P, T), & r(P) \leq r_c \\ G_c(P, T) \left[ \frac{\frac{2}{r^\gamma} - \frac{\gamma + 1}{r^\gamma}}{\frac{2}{r_c^\gamma} - \frac{\gamma + 1}{r_c^\gamma}} \right]^{1/2}, & r_c \leq r(P) < 1 \\ 0, & r(P) \geq 1 \end{cases} \quad (16)$$

In Eq. (16) the pressure ratio relative to the ambient pressure is:

$$r(P) = \frac{P_A}{P} \quad (17)$$

### 3.4 Prototype Facility results

The governing balance equations were discretized using a simple forward Euler time integration scheme. The prototype facility results were obtained by simulating 150 s, and the results are shown in Figure 1. The pressure behaves as expected, with an exponential decay type response, while the gas temperature has a much more complex behavior. The temperature is decreasing until approximately 50 s, at which point the temperature starts to increase. Clearly, over the first 50 s the temperature response is dominated by the energy exiting out the “break”. As the gas temperature decreases, the heat transfer rate with the wall increases until the heat transfer balances the energy leaving the break. The heat transfer rate then controls the temperature response until the end of the simulation.

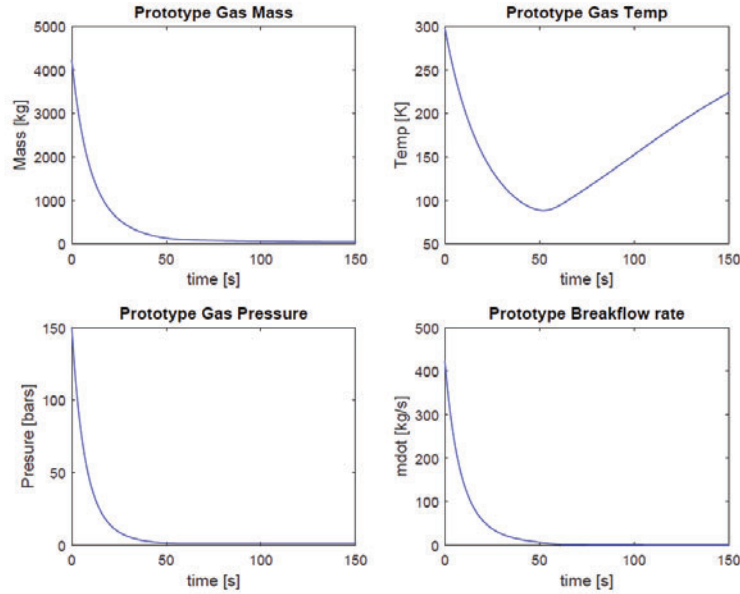


Figure 1. Prototype facility results

#### 4. SCALING ANALYSIS WITH DSS

##### 4.1 Normalized quantities

The pressure and temperature reference values were selected as their respective initial values. The normalized responses are written then as:

$$P = P^+ P_o, \quad T = T^+ T_o \quad (18)$$

Using notation consistent with Ref. [2], the agents-of-change on the pressure and temperature responses are:

$$\begin{aligned} \varphi_{out}^P &= R\gamma \frac{A_B}{V} G_{out} T, & \varphi_{out}^T &= (\gamma - 1) \frac{A_B}{V} G_{out} \frac{RT^2}{P} \\ \varphi_q^P &= (\gamma - 1) \frac{A_{SW}}{V} h_w (T_w - T), & \varphi_q^T &= (\gamma - 1) \frac{T}{P} \frac{A_{SW}}{V} h_w (T_w - T) \end{aligned} \quad (19)$$

Each of the agents of change are divided by the respective reference values to give the normalized agents of change. The dimensionless responses, in Eq. (18) are substituted into the terms in Eq (19) to yield:

$$\begin{aligned} \omega_{out}^P &= \frac{\varphi_{out}^P}{P_o} = R\gamma \frac{A_B}{V} G_{out} \frac{T}{P_o} = R\gamma \frac{A_B}{V} G_{out} \frac{T^+ T_o}{P_o} \\ \omega_q^P &= \frac{\varphi_q^P}{P_o} = \frac{(\gamma - 1)}{P_o} \frac{A_{SW}}{V} h_w (T_w - T) = \frac{(\gamma - 1)}{P_o} \frac{A_{SW}}{V} h_w (T_o - T^+ T_o) = \frac{(\gamma - 1)}{P_o} \frac{A_{SW}}{V} h_w T_o (1 - T^+) \end{aligned} \quad (20)$$

$$(21)$$

And the normalized agents of change on the temperature response are:

$$\omega_{out}^T = \frac{\varphi_{out}^T}{T_o} = \frac{(\gamma-1) A_B}{T_o} \frac{G_{out}}{V} \frac{RT^2}{P} = \frac{(\gamma-1) A_B}{T_o} \frac{G_{out}}{V} \frac{R(T^+T_o)^2}{P^+P_o} = R(\gamma-1) \frac{A_B}{V} G_{out} \frac{(T^+)^2 T_o}{P^+ P_o} \quad (22)$$

$$\omega_q^T = \frac{\varphi_q^T}{T_o} = \frac{(\gamma-1) T}{T_o} \frac{A_{SW}}{P} \frac{h_w}{V} (T_w - T) = \frac{(\gamma-1) T^+ T_o}{T_o} \frac{A_{SW}}{P^+ P_o} \frac{h_w}{V} (T_o - T^+ T_o) = (\gamma-1) \frac{T^+ T_o}{P^+ P_o} \frac{A_{SW}}{V} h_w (1 - T^+) \quad (23)$$

In Eqs. (21) and (23), the wall temperature was assumed to be a constant equal to the reference temperature value.

## 4.2 Similarity Criteria

The DSS similarity criteria, given by Eq. (3) is defined on the sum or aggregate agent of change via the effect parameter. The individual agents of change can have an arbitrary set of similarity criteria as long as the aggregate similarity criteria are satisfied [1]. The most restrictive requirement however is to enforce the same criteria on all agents of change. The individual agent of change similarity criteria are now used to determine constraints on the test facility design variables. The break flow agents of change similarity criteria are:

$$\lambda_A^P = \tilde{\Omega}_{out,R}^P = \tau_{S,R}^P \omega_{out,R}^P, \quad \lambda_A^T = \tilde{\Omega}_{out,R}^T = \tau_{S,R}^T \omega_{out,R}^T \quad (24)$$

The ratio of the model to prototype normalized break flow agents of change on their respective pressure responses is:

$$\omega_{out,R}^P = \left( \frac{A_B}{V} \right)_R \frac{G_{out,M}(t_{M,P}) T_M^+(t_{M,P}) T_{o,R}}{G_{out,P}(t_P) T_P^+(t_P) P_{o,R}} \quad (25)$$

In Eq. (25)  $t_{M,P}$  denotes the “scaled up” model reference time locations following the desired time scaling  $t_R = \tau_{S,R}^P = \lambda_A^P / \lambda_B^P$ :

$$t_{M,P} = \tau_{S,R}^P t_P \quad (26)$$

Substitute Eq. (25) into the break flow agent of change similarity criteria on the pressure response and rearrange to solve for the pressure response action ratio:

$$\tau_{S,R}^P = \lambda_A^P / \omega_{out,R}^P = \lambda_A^P \left[ \left( \frac{A_B}{V} \right)_R \frac{G_{out,M}(t_{M,P}) T_M^+(t_{M,P}) T_{o,R}}{G_{out,P}(t_P) T_P^+(t_P) P_{o,R}} \right]^{-1} \quad (27)$$

At the “scaled up” reference time locations, the model and prototype dimensionless responses can be related using the DSS coordinate transformation parameters:

$$\lambda_A^P = \frac{P_M^+(t_{M,P})}{P_P^+(t_P)}, \quad \lambda_A^T = \frac{T_M^+(t_{M,P})}{T_P^+(t_P)} \quad (28)$$

The pressure response action ratio simplifies to:

$$\tau_{S,R}^P = \frac{\lambda_A^P}{\lambda_A^T} \left[ \left( \frac{A_B}{V} \right)_R \frac{G_{out,M}(t_{M,P}) T_{o,R}}{G_{out,P}(t_P) P_{o,R}} \right]^{-1} \quad (29)$$

For the identity transformation,  $\lambda_A^P = \lambda_B^P = 1$ , and assuming fluid property similitude at full pressure, Eq. (29) reduces to  $(A_B/V)_R = 1$ . This is the classic power-to-volume methodology depressurization requirement that requires the break flow area to volume ratio be preserved.

Equation (29) was derived from the break flow agent of change on the pressure response. The same procedure could be repeated for the break flow agent of change on the temperature response. Although not presented here, the resulting expression on the temperature response action ratio would be identical to that given in Eq. (29). Therefore the following coordinate transformation constraint exists between the pressure and temperature responses:

$$\tau_{S,R}^P = \tau_{S,R}^T \rightarrow \frac{\lambda_A^P}{\lambda_B^P} = \frac{\lambda_A^T}{\lambda_B^T} \quad (30)$$

Since the action ratio is equivalent to the reference time scaling, the coordinate transformation constraint requires the pressure and temperature responses to have the same time scaling, relative to the prototype dynamics. In many respects this makes intrinsic sense since the temperature and pressure responses are coupled. Accelerating or decelerating the response of one will impact the other.

The pressure response action ratio can now be substituted into the heat transfer agent of change similarity criteria to yield a relationship between the break flow area and the wall surface area. The heat transfer similarity criteria on the pressure response is:

$$\lambda_A^P = \tilde{\Omega}_{q,R}^P = \tau_{S,R}^P \omega_{q,R}^P \quad (31)$$

The ratio between the model and prototype's heat transfer agents of change is:

$$\omega_{q,R}^P = \left( \frac{A_{SW}}{V} \right)_R \frac{h_{W,M}(t_{M,P}) (1 - T_M^+(t_{M,P})) T_{o,R}}{h_{W,P}(t_P) (1 - T_P^+(t_P)) P_{o,R}} \quad (32)$$

Substitute Eqs. (29) and (32) into Eq. (31):

$$\lambda_A^T = \frac{(A_{SW}/V)_R h_{W,M}(t_{M,P})/h_{W,P}(t_P) (1 - T_M^+(t_{M,P}))}{(A_B/V)_R G_{out,M}(t_{M,P})/G_{out,P}(t_P) (1 - T_P^+(t_P))} \quad (33)$$

Equation (33) is simply the ratio of the heat transfer to break flow agents of change. It is therefore analogous to a Pi-group from H2TS, except that the various terms in Eq. (33) are functions of time. Rearranging Eq. (33) provides a relationship between the break area to wall surface area as a function of prototype reference time:

$$\left( \frac{A_B}{A_{SW}} \right)_R = \frac{1}{\lambda_A^T} \frac{h_{W,M}(t_{M,P})/h_{W,P}(t_P)}{G_{out,M}(t_{M,P})/G_{out,P}(t_P)} \frac{(1-T_M^+(t_{M,P}))}{(1-T_P^+(t_P))} \quad (34)$$

The wall surface area is set by the tank height and diameter. Therefore, Eq. (34) can be used to determine the required test facility break flow area for given tank dimensions. If any of the ratios within Eq. (34) are not constant, the required test facility break area would change as a function of time. This is a fact that static similarity criteria from H2TS would not be able to capture. Another way to interpret this is, that if the break area must vary through time to preserve the similarity criteria, a fixed break area would induce distortion in the test facility.

Equation (34) will be evaluated assuming the prototype and test facility have choked flow out the break. Additionally, assume both facilities use the same gas with constant specific heats. Taking the ratio of the model to prototype critical mass flux in Eq. (15) at the corresponding “scaled up” references times yields:

$$G_{out,c,R} = \frac{P_M^+(t_{M,P})/P_P^+(t_P)}{(T_M^+(t_{M,P})/T_P^+(t_P))^{1/2}} \cdot \frac{P_{o,R}}{(T_{o,R})^{1/2}} = \frac{\lambda_A^P P_{o,R}}{(\lambda_A^T T_{o,R})^{1/2}} \quad (35)$$

Thus, as long as both facilities have choked flow conditions, the break mass flux ratio is a constant through prototype reference time.

Next, take the heat transfer coefficient ratio between the model and prototype assuming that both are within the turbulent flow regime:

$$\frac{h_{W,M}(t_{M,P})}{h_{W,P}(t_P)} = \frac{k_R}{H_R} \left( \frac{\overline{Nu}_M(t_{M,P})}{\overline{Nu}_P(t_P)} \right) = \frac{k_R}{H_R} \left( \frac{Gr_M(t_{M,P}) Pr_M}{Gr_P(t_P) Pr_P} \right)^d \quad (36)$$

Before substituting the Grashof and Prandtl number expressions into Eq. (36), rewrite the volumetric expansion coefficient and density evaluated at the film temperature as:

$$B_T = \frac{1}{T_{film}} = \frac{2}{T_W + T} = \frac{2}{T_o(1+T^+)} \quad (37)$$

$$\rho = \frac{P}{RT_{film}} = \frac{2P}{R(T_W + T)} = \frac{P_o}{RT_o} \frac{2P^+}{(1+T^+)} \quad (38)$$

Substitute Eqs. (37) and (38) into the Grashof number expression, and take the ratio of the model to prototype expressions. After rearranging and substituting in the normalized responses, Eq. (36) can be simplified to:

$$\frac{h_{w,M}(t_{M,P})}{h_{w,P}(t_P)} = (H_R)^{3d-1} \left( \frac{P_{o,R}}{T_{o,R}} \right)^{2d} \frac{(P_M^+(t_{M,P})/P_P^+(t_P))^{2d} \left[ \frac{(1-T_M^+(t_{M,P}))}{(1-T_P^+(t_P))} \right]^d}{\left[ \frac{(1+T_M^+(t_{M,P}))}{(1+T_P^+(t_P))} \right]^{3d}} \quad (39)$$

Note that for turbulent flow specifically,  $d=1/3$ , therefore the heat transfer coefficient ratio is independent of the height of the test facility. Applying the DSS transformations of the normalized responses allows writing the heat transfer coefficient ratio strictly as a function of the prototype reference time:

$$\frac{h_{w,M}(t_{M,P})}{h_{w,P}(t_P)} = \left( \frac{P_{o,R}}{T_{o,R}} \right)^{2/3} \frac{(\lambda_A^P)^{2/3} \left[ \frac{(1-\lambda_A^T T_P^+(t_P))}{(1-T_P^+(t_P))} \right]^{1/3}}{\left[ \frac{(1+\lambda_A^T T_P^+(t_P))}{(1+T_P^+(t_P))} \right]} \quad (40)$$

Substitute Eqs. (40) and (35) into the break area to wall surface area requirement:

$$\left( \frac{A_B}{A_{SW}} \right)_R = \frac{(\lambda_A^P P_{o,R})^{-1/3} \left[ \frac{(1-\lambda_A^T T_P^+(t_P))}{(1-T_P^+(t_P))} \right]^{4/3}}{(\lambda_A^T)^{1/2} (T_{o,R})^{1/6} \left[ \frac{(1+\lambda_A^T T_P^+(t_P))}{(1+T_P^+(t_P))} \right]^{1/3}} \quad (41)$$

The DSS transformation parameters can be specified by the designer. Therefore if  $\lambda_A^T = 1$ , Eq. (41) reduces to a constant through prototype reference time:

$$\left( \frac{A_B}{A_{SW}} \right)_R = \left( \lambda_A^P P_{o,R} (T_{o,R})^{1/2} \right)^{-1/3} \quad (42)$$

If the test facility height and diameter are specified, Eq. (42) allows the required test facility break area to be computed. As long as both the prototype and test facility have choked flow and turbulent heat transfer, a constant break area will satisfy the DSS similarity criteria.

### 4.3 Time Scaling

The action ratio given by Eq. (29) relates the time scaling to the break flow agent of change. For this specific application however, it is more convenient to write the time scaling as a function of the tank height and diameter. Using the heat transfer agent of change similarity criteria, substitute in the heat transfer coefficient ratio and simplify to yield:

$$\left( \frac{A_{SW}}{V} \right)_R = \frac{(\lambda_A^P P_{o,R} / T_{o,R})^{1/3}}{\tau_{S,R}^P} \quad (43)$$

Because the tanks are cylinders, the surface area to volume ratio between the model and prototype can be written in terms of the height and diameter ratios:

$$\left(\frac{A_{SW}}{V}\right)_R = \frac{(H + D/2)_R}{H_R D_R} \quad (44)$$

After substituting in Eq. (44) and rearranging Eq. (43) becomes:

$$\tau_{S,R}^P = \frac{H_R D_R \left(\lambda_A^P P_{o,R}/T_{o,R}\right)^{1/3}}{(H + D/2)_R} \quad (45)$$

As the height and diameter shrink relative to the prototype, the test facility dynamics will be accelerated. The denominator in Eq. (44) is a representation of the tank aspect ratio. As that ratio decreases it tends to decelerate the dynamic response of the test facility. The tank geometry therefore has several competing effects. Decreasing the initial pressure of the test facility also accelerates the dynamics, however the heat transfer correlation exponent decreases the pressure scaling's direct impact on the time scaling.

#### 4.4 Optimal Reference Time Interval

The proceeding discussion had one key assumption, that the model was in fact ideally scaled relative to the prototype. That assumption allowed the action ratio to equal the reference time ratio, which ultimately led to Eq. (45). In order for the action ratio and thus the reference time ratio given by Eq. (45) to hold throughout the transient, Eq. (33) must be satisfied throughout the model's transient. As shown in Section 4.2, as long as both facilities have choked flow out the break the, the break area to wall surface area ratio (Eq. (34)) is a constant through reference time. Therefore, it is expected that as long as both facilities have choked flow, the model will be ideally scaled.

Given this concept, any distortion is expected to occur once the test facility transitions from choked to unchoked flow out the break. Since both the model and prototype have the same ambient pressure, a reduced pressure test facility will transition to unchoked flow "sooner" than it is supposed to. If the break area is fixed, the heat transfer agent of change will increase relative to the break flow agent of change, resulting in different dynamics relative to the prototype. This distortion alters the time scaling compared to the ideally scaled time scale.

For these reasons, the model's 'optimal' reference time interval must be identified. The model's response is then compared to the prototype's response over this 'optimal' reference time interval. The reference time interval is 'optimal' in the sense that the action ratio equals the reference time ratio over that interval. The procedure for determining the 'optimal' reference time interval is exactly the same as the procedure described in [5]. The procedure is not described in this paper and so the interested reader should consult [5] for details.

The 'optimal' reference time interval essentially provides a check on the assumptions used to determine Eqs. (45) and (42). If the assumptions were valid, the 'optimal' reference time

interval will equal the ideally scaled reference time interval. If the assumptions however were not valid over the duration of the transient, the ‘optimal’ reference time interval will be different from the time scaling predicted by Eq. (45).

## 5. TEST FACILITY OPTIMIZATION

### 5.1 Design Variable Search Matrix

A simple search over possible design variables is used as the optimization algorithm. A more rigorous optimization scheme could be used, but this simple search is adequate for the demonstration of the DSS methodology. The design variables are the height ratio,  $H_R$ , diameter ratio,  $D_R$ , and initial pressure ratio,  $P_{o,R}$ . Table 1 below provides the list of values for each of the design variables used in this work. All combinations of the design variables were analysed, yielding a total of 36 design options considered in this work.

Table 1: Design Variable Search Matrix

Design Variable	Values Considered			
$P_{o,R}$	1	0.75	0.5	
$H_R$	0.25	0.5	0.75	1
$D_R$	0.25	0.5	0.75	

### 5.2 Design Procedure

For a specific height and diameter ratio, the wall surface area ratio is computed. The DSS transformation parameters,  $\lambda_A^T$  and  $\lambda_A^P$  were both set to unity. The required break area over the choked flow portion the transient is computed using Eq. (42) and the specific design’s pressure ratio. Note that the initial temperature ratio was assumed equal to 1 for all design options. The break area was then held constant throughout the entire transient.

The model’s response was then simulated using the same Forward Euler scheme as the prototype. The ‘optimal’ reference time interval was determined using the model’s pressure response over its whole transient. The model’s dimensionless coordinates were then computed over the ‘optimal’ reference time interval. In order to  $\eta_\chi(\tilde{\tau})$ , the  $\lambda_A^P$ -value was then recalculated by taking the ratio of the effect parameters. For a distorted design, the  $\lambda_A^P$ -value is not constant over the model’s ‘optimal’ reference time interval, therefore the mean value was used to compute  $\eta_\chi(\tilde{\tau})$  with Eq. (5). The total distortion,  $\eta_T$ , was then determined by numerically evaluating the integral in Eq. (6).

The designs are compared using the total distortion computed from the pressure response. The pressure response does not have a minimum value during the transient. Focusing on the temperature response requires dividing the transient into several time phases to avoid this minimum point. Finding the design with the minimal pressure total distortion is equivalent to finding the design with the minimal total distortion with respect to the total system energy. Additionally, focusing on the pressure response

### 5.3 Dimensional Results

Each of the various test facility temperature and pressure responses are compared to the prototype in Figure 2. It is clear that all of the designs have accelerated responses relative to the prototype. The dots on the prototype's temperature response in chronological order correspond to 99% of the total temperature decrease before reaching the minimum point, the "symmetric" temperature value after the temperature starts increasing, and the temperature at the end of the transient. The dots on the models' temperature responses correspond to those same temperatures, but at the "scaled up" model reference time locations. The dots on the models' pressure responses mark the end of the 'optimal' reference time interval.

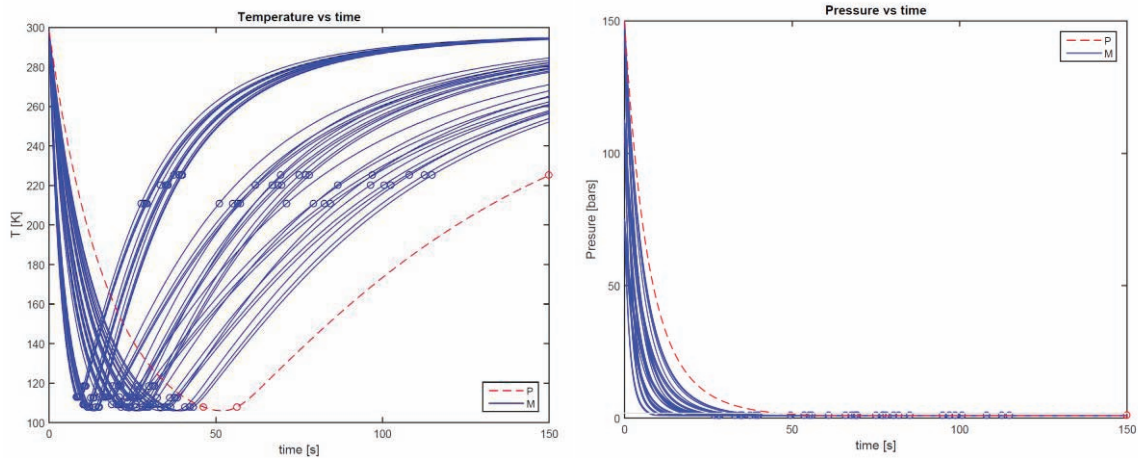
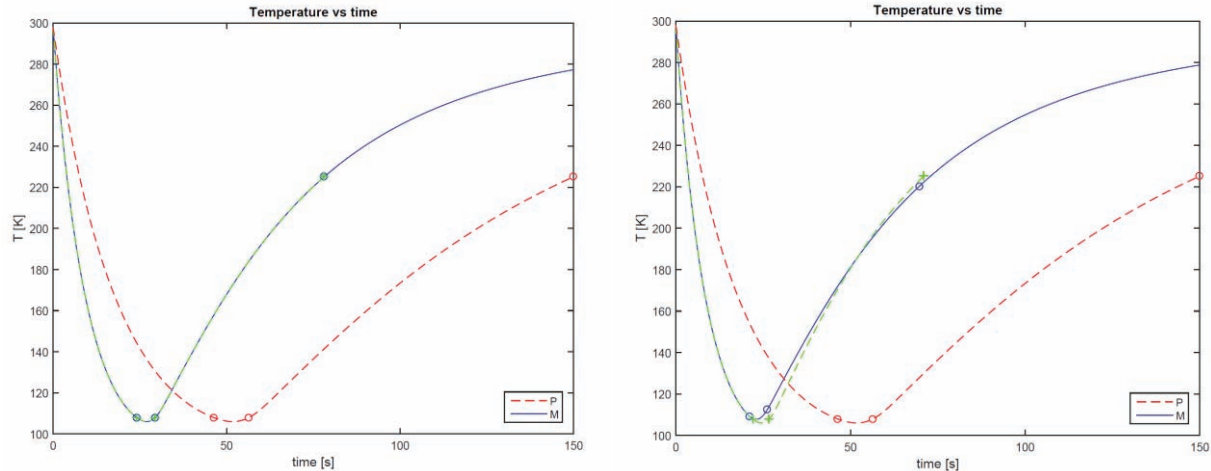


Figure 2. Test facility and prototype temperature and pressure responses

Although difficult to see in Figure 2, the minimum temperature values depend on the pressure scaling. Full pressure test facilities have the same minimum temperature value as the prototype, while reduced pressure test facilities have a higher temperature value as the minimum point. The reason is because the reduced pressure test facilities transition to unchoked flow "sooner" than the prototype, as described in Section 4.4. To illustrate this, two specific designs are compared in Figure 3. The left plot shows the temperature response for a full pressure facility with  $H_R = 1$  and  $D_R = 0.5$ . The right plot shows the temperature response for a reduced pressure facility with  $P_{o,R} = 0.75$  and the same height and diameter ratio as the facility on the left plot in Figure 3. In both the left and right plots, the dashed green curves are the ideally scaled temperature responses computed by directly transforming the prototype response. As seen on the left, the actual model's response falls directly on top of the ideally scaled, transformed response. The reduced pressure facility's response however does not match up exactly with the ideally scaled, transformed response, as shown in the right hand side plot. The reduced pressure test facility heats up faster than it is ideally supposed to, because the unchoked flow out the break removes less energy than if the flow was choked.



**Figure 3. Test facility temperature responses (Left: full pressure facility, Right: reduced pressure facility)**

The distortion in the reduced pressure facilities is effectively compressing the ideal reference time scaling. Figure 4 shows the ideal reference time ratio on the  $x$ -axis and the estimated reference time ratio, as computed from the ‘optimal’ reference time interval on the  $y$ -axis. The marker type denotes the pressure ratio and the marker color denotes the height ratio for each of the design options. A dotted black line along the diagonal denotes when the two are equal and only the full pressure test facilities fall on top of this line. The lower the initial pressure, the more pronounced the difference becomes between the two time ratios.

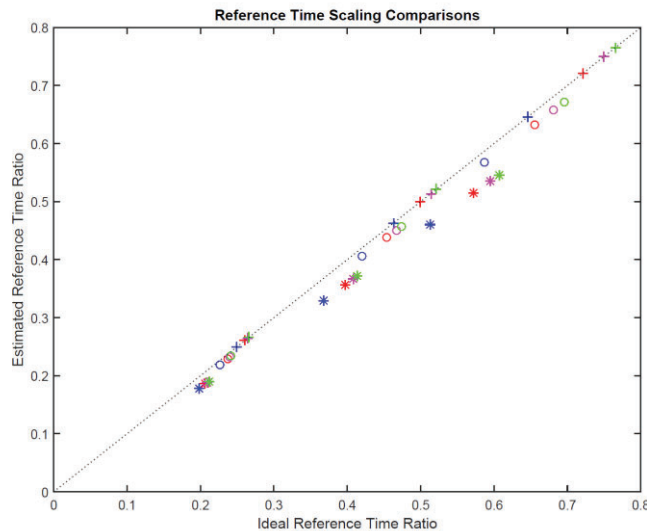


**Figure 4. Ideal vs estimated reference time scaling**

#### 5.4 DSS Dimensionless Process Curves

The test facility pressure responses over their respective ‘optimal’ reference time intervals are synthesised using the DSS geodesic process curves in Figure 5. The blue curves correspond to the test facilities, while the dashed red curve is the prototype. Three distinct clusters are present with all 12 full pressure models collapsing on top of the prototype process curve. The two other

clusters correspond to the reduced pressure test facility designs. The cluster furthest from the prototype is the set of designs with the lowest initial pressure.

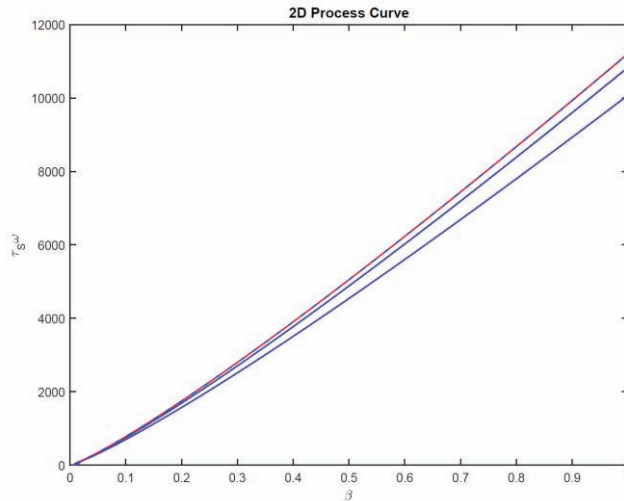


Figure 5. Pressure response 2D process curves

### 5.5 DSS Total Distortion

The total distortion for each of the 36 design options are shown in Figure 6. The  $x$ -axis is the break area to volume ratio relative to the prototype, which gives an indication for the time scaling for each design. The higher the break area to volume ratio, the more accelerated the design is relative to the prototype. The same marker type and color conventions used in Figure 4 are used in Figure 6. As visualized in the 2D process curves, the total distortion is directly proportional to the initial pressure ratio. The full pressure test facilities with the fastest time dynamics (those with the largest  $(A_B/V)_R$  values) do not have a total distortion of identically zero, in Figure 6. Although not shown in this paper, this slight distortion is due to numerical error in the Forward Euler time integration scheme. Even with a timestep of half a millisecond, there is still enough numerical error in the fastest time dynamics to induce slight distortion relative to the prototype's response over the entire transient. However, this numerical distortion is very small relative to the distortion induced by reducing the initial pressure and keeping a fixed break area. The distortion is therefore nearly independent of the physical size of the test facility, as long as the break area satisfies the DSS similarity criteria. To allow the reduced pressure test facilities to also be ideally scaled, the break area must change through time as specified by Eq. (34).

If H2TS had been used in this analysis instead of DSS, the  $\Pi$ -groups would need to have been estimated. Since the heat transfer rate is initially zero, a reference value would need to be chosen in order to compute the heat transfer rate  $\Pi$ -group. If the average heat transfer rate was used, the heat transfer term would be considered to have negligible impact on the pressure response. No aspect of the test facility design would need to consider the heat transfer agent of change. DSS however allowed the heat transfer agent of change to impact the required break area scaling.

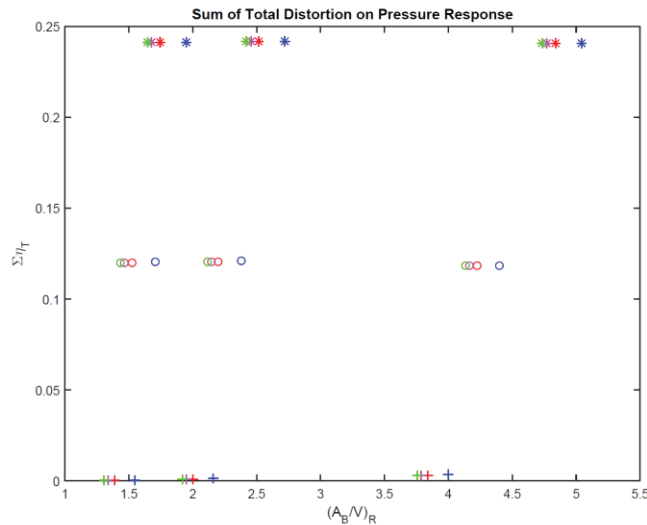


Figure 6. Sum of total distortion on temperature (left) and pressure (right) responses for all designs considered

## 6. CONCLUSIONS

The DSS methodology provides a powerful framework to incorporate the impact of the transient dynamic behaviour into the scaling analysis. As this work showed, the DSS similarity criteria allows identifying how specific design choices may impact the distortion. Although only a simple gas blowdown transient was analysed here, the concepts of identifying how design variables should change through time to preserve process similarity have real applications to real test facility designs. The DSS methodology provides the tools to try and quantify those effects to aid designers.

## 7. REFERENCES

- [1] J. N. Reyes, "The Dynamical System Scaling Methodology," in *The 16th International Topical Meeting on Nuclear Reactor Thermal Hydraulics (NURETH-16)*, Chicago, IL, USA, 2015.
- [2] J. Reyes, C. Frepoli and J. Yurko, "The Dynamical System Scaling Methodology: Comparing Dimensionless Governing Equations With the H2TS and FSA Methodologies," in *The 16th Internal Topical Meeting on Nuclear Reactor Thermal Hydraulics (NURETH-16)*, Chicago, IL, 2015.
- [3] J. N. Reyes and L. Hochreiter, "Scaling for the OSU AP600 test facility (APEX)," *Nuclear Engineering and Design*, vol. 186, pp. 553-109, 1998.
- [4] A. Petruzzi, D. Cacuci and F. D'Auria, "Best Estimate Model Calibration and Prediction Through Experimental Data Assimilation II: Application to a Blowdown Benchmark Experiment," *Nuclear Science and Engineering*, vol. 165, pp. 45-100, 2010.
- [5] C. Frepoli and J. Yurko, "Experimental Test Facility Data Synthesis with the Dynamical System Scaling Methodology," in *The 16th International Topical Meeting on Nuclear Reactor Thermal Hydraulics (NURETH-16)*, Chicago, IL, 2015.